Electro-plating and characterisation of cadmium sulphide thin films using ammonium thiosulphate as the sulphur source

ABDUL-MANAF, N.A., WEERASINGHE, A.R., ECHENDU, O. K. and DHARMADASA, I. M. <http://orcid.org/0000-0001-7988-669X>

Electro-plating and characterisation of Cadmium Sulfide thin films using Ammonium Thiosulfate as the sulphur source

N.A. Abdul-Manaf[1*], A.R. Weerasinghe[12], O.K. Echendu[13] and I.M. Dharmadasa[1]
[1]Electronic Materials and Sensors Group, Materials and Engineering Research Institute, Faculty of Arts, Computing, Engineering and Sciences, Sheffield Hallam University,
Sheffield S1 1WB, United Kingdom.
[2]Dept. of Mechanical Engineering, California State University, Fresno 2320 E. San Ramon M/S EE94 Fresno, CA 93740, USA
[3]Department of Physics, Federal University of Technology, P. M. B. 1526, Owerri, Nigeria
Email: azlian_manaf@yahoo.co.uk
Tel: +44(0)1142256910
Fax: +44(0)1142256930

Abstract:

Cadmium sulfide (CdS) thin films have been successfully prepared from an aqueous electrolyte bath containing $CdCl_2$ and ammonium thiosulfate ($(NH_4)_2S_2O_3$) using electrodeposition technique. The structural, compositional, optical, morphological and electrical properties of these thin films have been characterized using X-ray diffraction (XRD), Raman spectroscopy, energy dispersive X-ray (EDX) spectroscopy, UV-Vis spectrophotometry, scanning electron microscopy (SEM), atomic force microscopy (AFM), photoelectrochemical (PEC) cell and D.C. current-voltage (I-V) measurements. The optimum deposition cathodic potential has been observed at 1455 mV, in a 2-electrode system with respect to carbon anode. Structural analysis using XRD shows a mixture of hexagonal and cubic phases in the as-deposited CdS samples and a phase transformation to the hexagonal structure occurred after heat treatment at 400^{o}C for 20 min.. Optical studies demonstrate an improvement in the band edge, producing 2.42 eV for the band gap of the films after heat treatment. The heat treated CdS thin films show better transmission for wavelengths longer than 500 nm. SEM and AFM show that the heat-treated samples are more uniform, smoother and have larger grain size. Electrical studies confirm that the CdS thin films have n-type electrical conductivity and heat treated CdS thin films have resistivities of the order of 10^5 Ωcm.

Keywords: CdS, $(NH_4)_2S_2O_3$, electrodeposition, thin films

1. INTRODUCTION

In recent years, the deposition of CdS films has become increasingly important due to their applications in many industrial fields. CdS is an n-type semiconductor with a wide direct band gap of 2.42 eV for bulk material at room temperature [1]. These layers demonstrate a good conversion efficiency (above 21%) when employed as a window layer in combination with absorber materials such as CdTe [2, 3] and CIGS ($CuInGaSe_2$) [1]. Therefore, CdS thin films have been used widely as window layers in solar cells. CdS thin films have been deposited by various methods such as dip coating [4], chemical bath deposition (CBD) [5, 7], spray pyrolysis [3, 6], vapour deposition [7] and electrodeposition [7,8,9]. Electrodeposition is an attractive technique for the preparation of CdS because it uses relatively inexpensive instruments, enables deposition of large area films and provides easier control of growth parameters such as applied voltage, current density, pH and temperature of the electrodeposition electrolyte. It also offers a continuous industrial process drastically reducing toxic waste generation compared to batch process of CBD since the electrolyte can be used over a long period of time [7].

A highly crystalline structure, higher optical transmission in wavelength >512 nm, having wide optical band gap with n-type electrical conductivity, films with minimum defects, lower thickness (<200 nm) and highly uniform layers are the fundamental requirements for solar cell window layers [7]. In order to meet these requirements, CdS thin films should be grown in desired environments without harmful impurities. In the case of electroplating, $Na_2S_2O_3$ is normally used as a sulphur source [2, 7, 8, 9]. Although sodium (Na) ions are not electrodeposited at low cathodic voltages, Na can be incorporated in CdS films via absorption or adsorption and chemical reactions as Na accumulates in the bath where $Na_2S_2O_3$ is gradually added to the electrolyte. Na is a p-type dopant in CdS [1], and it can increase the electrical resistivity of n-CdS layers introducing detrimental effects for solar cell application. In order to avoid this situation, $(NH_4)_2S_2O_3$ has been used as the sulphur source in this research. With this precursor, CdS layers can be grown continuously with a long bath lifetime, avoiding accumulation of harmful elements such as Na. This paper presents the results obtained in growth and characterisation of CdS layers by electro-plating using $(NH_4)_2S_2O_3$ as sulphur precursor.

2. EXPERIMENTAL METHOD

All chemicals and substrates used in this study were purchased from Sigma Aldrich. Hydrated cadmium chloride ($CdCl_2 \cdot xH_2O$) with purity of 98% and ammonium thiosulfate $(NH_4)_2S_2O_3$ of analytical reagent grade were used as precursors. $(NH_4)_2S_2O_3$ required stirring for 2 hours at 100^{o}C before it fully dissolved in water. The $CdCl_2$ aqueous solution was electro-purified for 100 hours before the experiment started. The working electrode, fluorine-doped tin oxide (FTO)-coated glass substrates with sheet resistance of 7 Ω/□ were cut into 2 x 2 cm^2 pieces. The cleaning process started by rinsing the substrates in soap solution, rinsing in de-ionized water and immersing them in acetone solution. These were then rinsed thoroughly in de-ionized water and dipped in methanol solution. The substrates were then rinsed in de-ionized water before electrodeposition.

CdS thin films were electrodeposited from an acidic aqueous solution containing 0.3M $CdCl_2$ and 0.03M $(NH_4)_2S_2O_3$ in 300 ml of de-ionized water. A two-electrode system with graphite as anode and a FTO coated glass substrate as working electrode were used for this study. The electrolytic bath was continuously stirred and the temperature was kept constant at 85±2^{o}C. The pH was maintained at 2.00±0.02 and dilute solutions of HCl and NH_4OH were used to control the pH at the start of the deposition. The overall reaction for the formation of CdS at the cathode can be described as follows:

$$Cd^{2+} + S_2O_3^{2-} + 2e^- \rightarrow CdS + SO_3^{2-}$$

Before the layer deposition, a cyclic voltammogram was obtained in order to estimate the approximate voltage range for film deposition. Using the voltage range estimated, CdS thin films were grown at different growth voltages (V_g) and the growth conditions were optimized after characterization. The structural properties of CdS thin films deposited on glass/FTO substrates were characterized using X-ray diffraction (XRD) and Raman spectroscopy. The XRD measurements were carried out using X'pert pro-diffractometer with a Cu-Kα excitation wavelength of 1.541 Å, while Raman spectroscopy was carried out with a Renishaw Raman microscope with a CCD detector and 514 nm argon ion laser source. Composition of CdS thin films were characterized using energy dispersive X-ray (EDX). The EDX measurements were carried out using EDX detector attached to the FEI NOVA NANO SEM. Optical properties were measured using a Cary 50 scan UV-Vis spectrophotometry to determine the absorption and transmittance properties of the electrodeposited layers. The morphology, grain size and surface roughness of CdS thin films were observed using scanning electron microscopy (SEM) and atomic force microscopy (AFM). The SEM images were taken using the same FEI NOVA NANO SEM system, while AFM measurements were carried out using ISPM-5200 System (JEOL, Tokyo, Japan). Electrical properties were studied using D.C. electrical conductivity measurements and photo-electrochemical (PEC) cell measurements. The D.C. electrical conductivity measurements were carried out using a fully automated I-V system including a Keithley 619 electrometer & multimeter, while the photo-electrochemical (PEC) cell method was carried out using an electrolyte of 0.1M $Na_2S_2O_3$. The thicknesses were measured using an optical profilometer and the theoretical estimation of thicknesses was carried out using Faraday's laws of electrolysis.

3. RESULTS AND DISCUSSION

3.1 Voltammogram

Voltammogram provides the information on electric current flow in the electrochemical bath and it is obtained by measuring the current passing through the working electrode during the potential scans. Fig. 1 shows a typical cyclic voltammogram of aqueous solutions of (a) 0.3M $CdCl_2$, (b) 0.03M $(NH_4)_2S_2O_3$ and (c) mixture of 0.3M $CdCl_2$ and 0.03M $(NH_4)_2S_2O_3$ during the forward and reverse cycles between 0 and 2500 mV. The scanning rate was fixed at 3 mVs^{-1} and the bath temperature was kept constant at 85^{o}C.

From Fig. 1(a), it is noted that Cd from $CdCl_2$ source started to deposit in the forward cycle at a cathodic voltage of around 1049 mV. Cd has a reduction potential of E_o = -400 mV [10]. As the voltage increases, the current density increases and thus more Cd is deposited. In a reverse sweep, the layer starts to dissolve at a cathodic voltage of around 1579 mV. In Fig. 1(b), the reduction of $S_2O_3^{2-}$ is observed at 488 mV, thus suggesting that sulfur is depositing at a lower cathodic potential compared to Cd. Sulphur has a reduction potential of E_o = +480 mV [10].

From the voltammogram of a mixture of 0.3M $CdCl_2$ and 0.03M $(NH_4)_2S_2O_3$ shown in Fig. 1(c), one notices a single clear hump at cathodic potential starting at ~875 mV which is associated with the co-deposition of Cd and S atoms to form a mixture of sulphur and cadmium sulfide. Also, it is observed that the film colour starts changing to transparent yellow at cathodic growth voltages (V_g) ≥500 mV which suggests a sulfur rich region. These films start turning to transparent greenish-yellow at cathodic voltage of ~1100 mV and above, thus suggesting the presence of stoichiometric CdS. As the potential increased to ≥ 1600 mV, the film colour becomes dark green in appearance which suggests that the Vg≥ 1600 mV are in the Cd-rich region. CdS thin films with a

good dark yellow appearance can be grown at the growth potentials from 1100 mV to 1500 mV. Changing the applied potential can vary the composition of the formed CdS compound [9]. Therefore, the stoichiometry of CdS thin film is predictable, showing sulfur-rich materials at lower cathodic potentials and cadmium-rich films at higher cathodic potentials. The detailed study on the cathodic potential from 1100 to 1500 mV was carried out to obtain the best V_g to grow CdS thin films. After growing at different voltages and characterization with XRD, this voltage region was narrowed down to 1440-1460 mV.

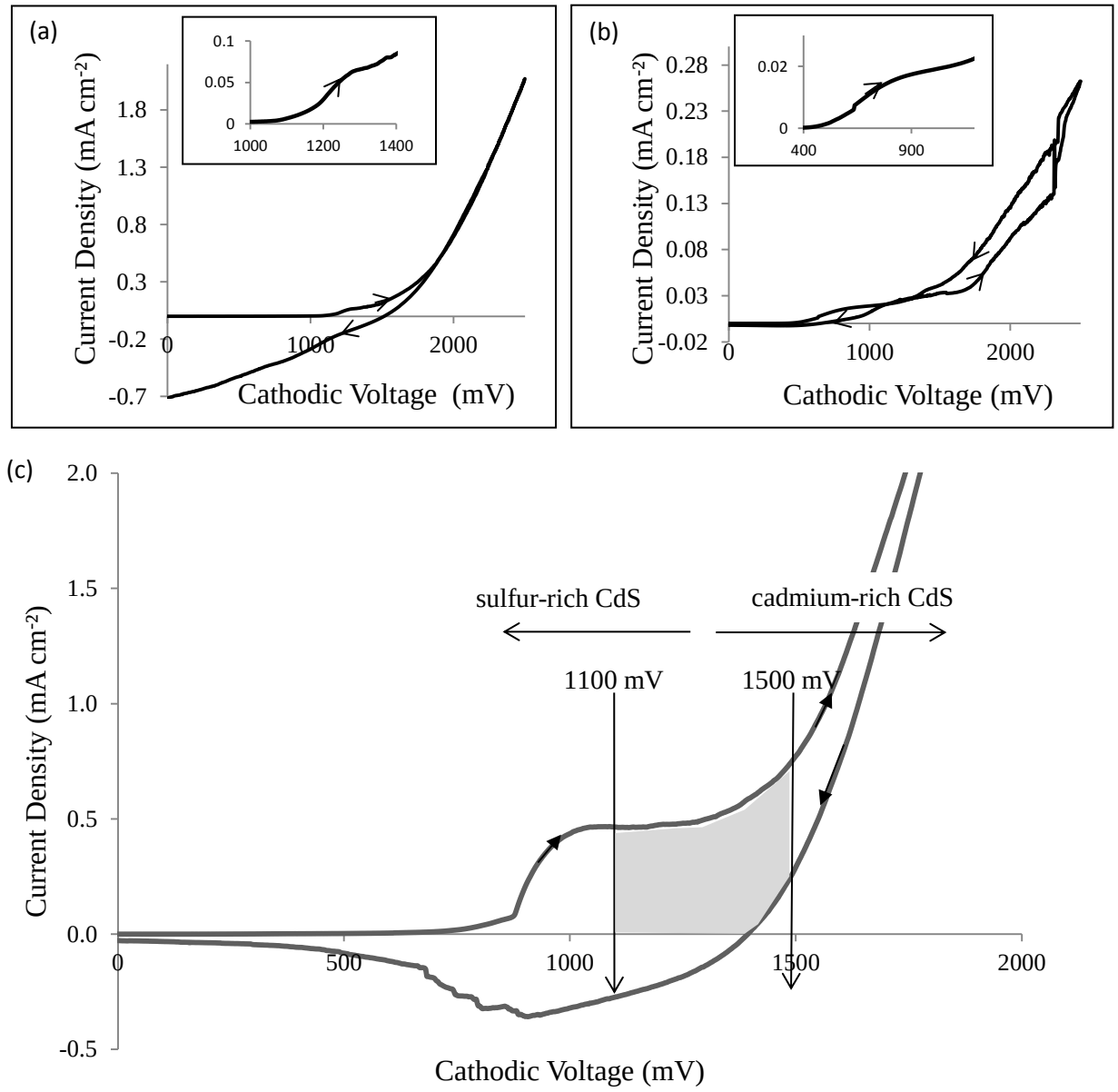

Fig. 1 Cyclic voltamogram for aqueous solutions of (a) 0.3M $CdCl_2$, (b) 0.03M $(NH_4)_2S_2O_3$ and (c) mixture of 0.3M $CdCl_2$ and 0.03M $(NH_4)_2S_2O_3$ using glass/FTO as the cathode and a graphite rod as the anode. The arrows indicate the directions of the cycles

For a continuous plating process, it is important to establish a stable electrolyte bath. If more sulfur has been added to the bath, precipitation is observed at room temperature. However, this problem had been solved by reducing the pH to a suitable range, heating up the bath and growing at higher temperature ($\geq 85^{o}$C), and reducing the concentration of S precursor. These approaches are really help to minimize the unwanted precipitation and maintain the stability of CdS bath for a longer time.

3.2 Structural analysis

3.2.1 X-ray diffraction

In this work, CdS thin films were grown at different cathodic potentials from 1440 mV to 1460 mV. The study on cathodic potential was done by referring to the best crystallinity as observed in XRD for as-deposited and heat treated layers. The XRD patterns of the as-deposited and heat-treated CdS layers are shown in Fig.s 2(a) and (b) respectively. According to the as-deposited samples in Fig. 2(a), the appearance of small crystalline peaks of CdS at 2θ = 24.93° and 28.46° corresponding to the (100) and (101) hexagonal planes. An intense hexagonal CdS peak (002) overlaps with FTO peak at 2θ = 26.67°. Also a small crystalline peak of sulphur (S) at 2θ = 32.22° and cubic CdS at 2θ = 30.81° and 43.91° were observed, corresponding to diffraction of (200) and (220) planes respectively. Thus, verifying that as-deposited CdS thin films are polycrystalline in nature with mixed phases. Heat treatment typically reduces the excess sulphur and causes phase transition from the mixture of cubic and hexagonal phase to single hexagonal phase. It is well known that CdS can grow in two crystalline structures that are cubic (zinc blende) and hexagonal (wurtzite) [4]. Between these two crystalline structures, the hexagonal structure is the thermodynamically more stable while cubic CdS with zinc blende structure is a metastable phase [4]. The formation of a particular CdS thin film structure is dependent on the preparation conditions [1, 11, 12]. Kaur et al. [8] reported that the CdS films exhibit hexagonal and cubic structures due to vigorous stirring during the electrodeposition [11].

Fig. 3 shows the XRD spectra plotted in log-scale in order to identify all peaks. These spectra are for as-deposited and heat-treated CdS layers grown at V_g = 1455 mV. The three peaks of hexagonal CdS show an obvious enhancement in crystallinity after heat-treatment. This is probably because of the reduction of strain in the film due to some degree of reorientation of the particles during the heat treatment process [12]. The summary of XRD data and obtained structural parameters of CdS thin films grown at V_g 1455 mV are shown in Table 1. The crystallite size, D was calculated using the Scherrer's formula:

$$D = \frac{0.94\,\lambda}{\beta \cos\theta} \qquad \ldots(1)$$

where λ is the wavelength of the X-rays used (1.541 Å), β is the full width at half maximum (FWHM) of the diffraction peak in radian and θ is the Bragg angle.

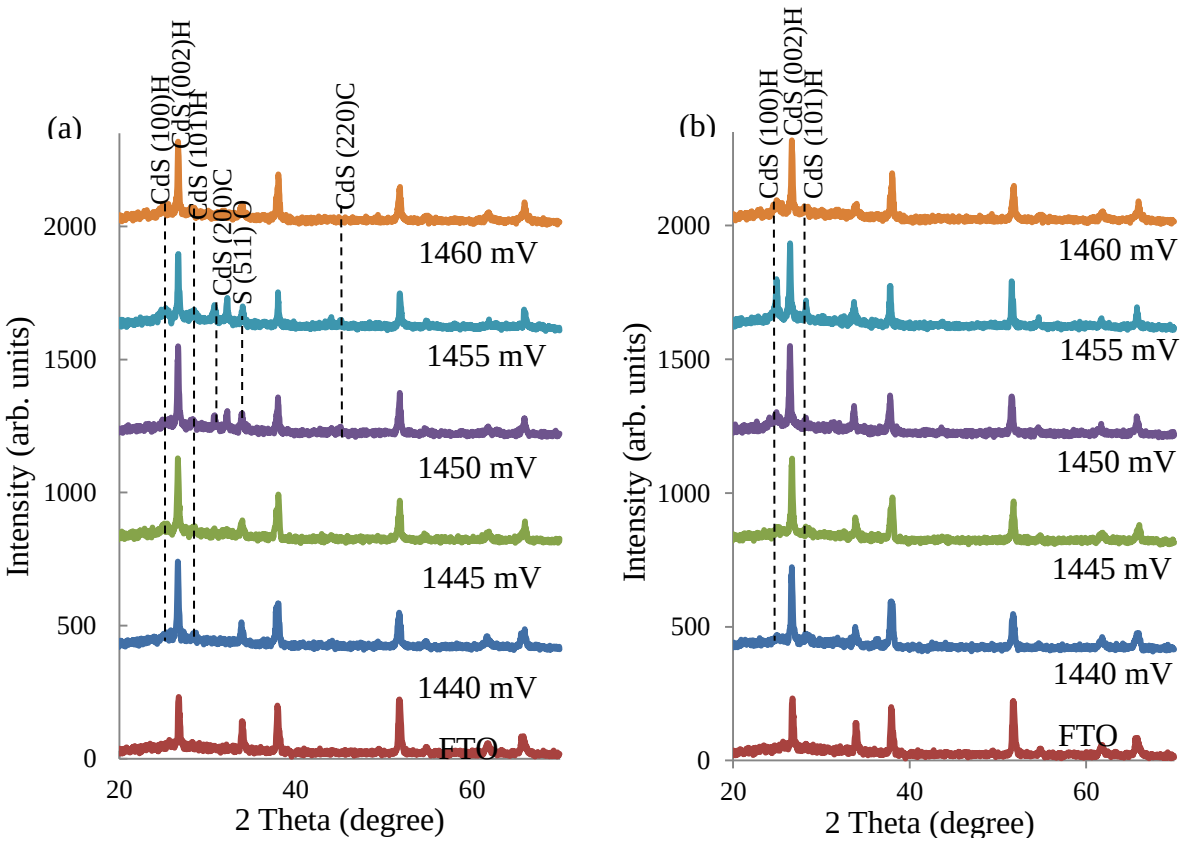

Fig. 2 XRD patterns of CdS thin films grown at cathodic voltage range of 1440 to 1460 mV (a) for as-deposited and (b) for heat treated at 400°C in air. Note that the growth duration for all layers was 60 min.

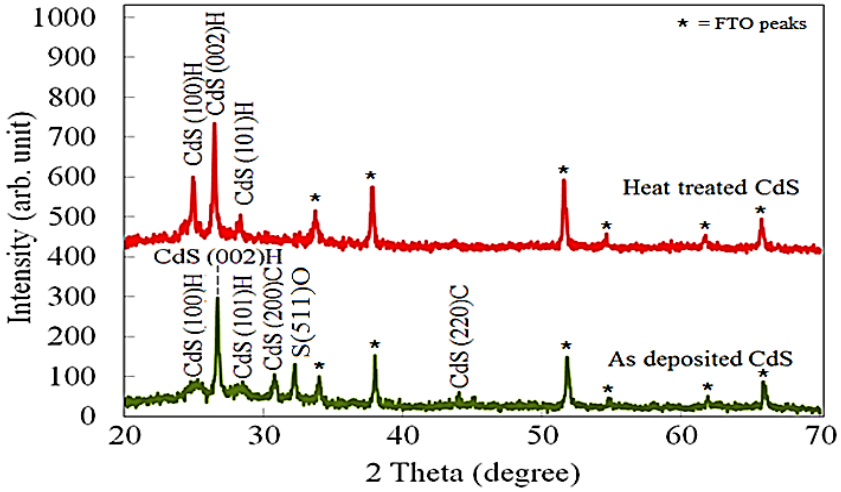

Fig. 3 XRD patterns of CdS layer grown at 1455 mV plotted in log-scale

Table 1 Summary of XRD data for as-deposited and heat treated CdS grown at 1455 mV

Sample	Angle (*2θ*)	Intensity relative to the peak at ~26° (%)	FWHM (Degrees)	Plane of orientation (h k l)	Crystallite size, *D* (nm)	d- spacing (Å)	Assignments
As-deposited CdS (V_g = 1455 mV)	24.93	8.9	0.779	(1 0 0)	11.7	3.56	Hex CdS
	26.67	100.0	0.197	(0 0 2)	47.0	3.34	Hex CdS/FTO
	28.46	7.8	0.322	(1 0 1)	29.3	3.11	Hex CdS
	30.81	19.2	0.325	(2 0 0)	29.7	2.90	Cubic CdS
	32.22	33.7	0.213	(5 1 1)	45.9	2.78	Orthorhombic S
	43.91	5.1	0.325	(2 2 0)	35.5	2.32	Cubic CdS
Heat treated CdS (V_g = 1455 mV)	24.86	48.5	0.279	(1 0 0)	32.7	3.58	Hex CdS
	26.46	100.0	0.162	(0 0 2)	57.1	3.37	Hex CdS/FTO
	28.15	27.9	0.265	(1 0 1)	35.6	3.17	Hex CdS

3.2.2 Raman spectroscopy

Raman spectroscopy is an alternative method to identify material phases and determine the degree of crystallinity of the thin films. The excitation source used in this work was 514 nm argon ion laser and typical Raman spectra for as-deposited and heat-treated CdS layers are shown in Fig. 4. The dominant peaks in the spectra are the longitudinal optical (LO) vibration mode at wave numbers 305 cm^{-1} for 1LO and 605 cm^{-1} for 2LO (Fig. 4). Both films show clear peaks at 1LO with a small blue shift in peak positions after heat treatment. Ichimura et al. [13] reported that increase of Raman shift is due to enlargement in crystallite size. This trend is consistent with the XRD results shown in Table 1 and microstructural studies shown in Fig. 11 and 12. The FWHM of Raman spectra is also used to evaluate qualitatively the crystallinity of CdS. The heat treated sample shows a decrease in the FWHM of 1LO and 2LO peaks which indicate an improvement in the crystallinity of thin films.

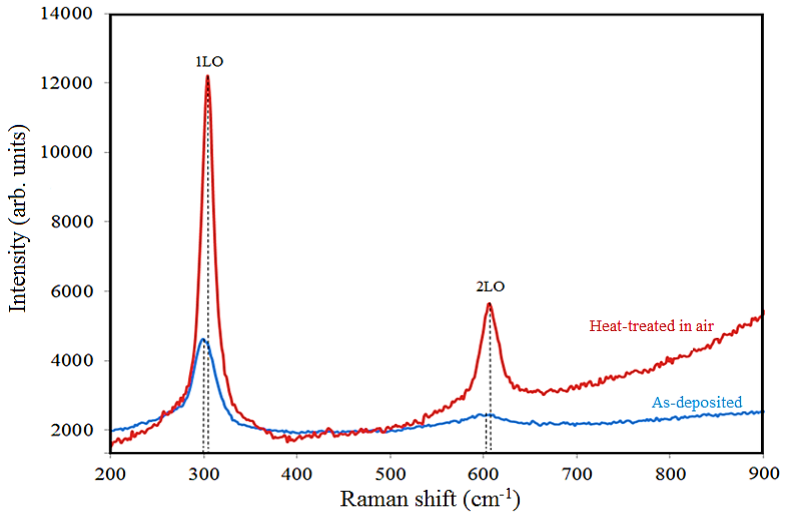

Fig. 4 Raman spectroscopy of as-deposited and heat treated (at 400°C for 20 min in air) CdS thin films

Table 2 Analysis of Raman peak positions, peak intensities and FWHM values

	As-deposited		Heat treated	
	1LO	2LO	1LO	2LO
Raman peak position (cm^{-1})	300	600	304	605
Intensity (a.u.)	2309	217	10393	2477
FWHM (cm^{-1})	31.97	42.07	16.83	23.62

3.3 Compositional characterisation

The EDX measurement has been used to confirm the composition and atomic percentage of CdS thin films. Fig. 5 shows the spectra of (a) as-deposited and (b) heat-treated CdS. The spectra indicate the presence of both Cd and S atoms in these materials. The peaks also show the presence of O, Si, and Sn which come from the underlying substrate (glass) and conducting layer (FTO), on which these CdS layers were grown. The percentage atomic concentrations of Cd and S in these samples are presented in Table 3. It is observed that the as deposited sample is S-rich. The heat-treated CdS shows less concentration of S in the layer, which revealed that the sample become more stoichiometric after heat treatment.

Table 3: Compositions of as-deposited and heat-treated CdS thin films.

Sample	Atomic composition %		Cd/S ratio
	Cd	S	
As-deposited	46.4	53.6	0.87
Heat-treated at 400°C, 20 min.	47.0	53.0	0.89

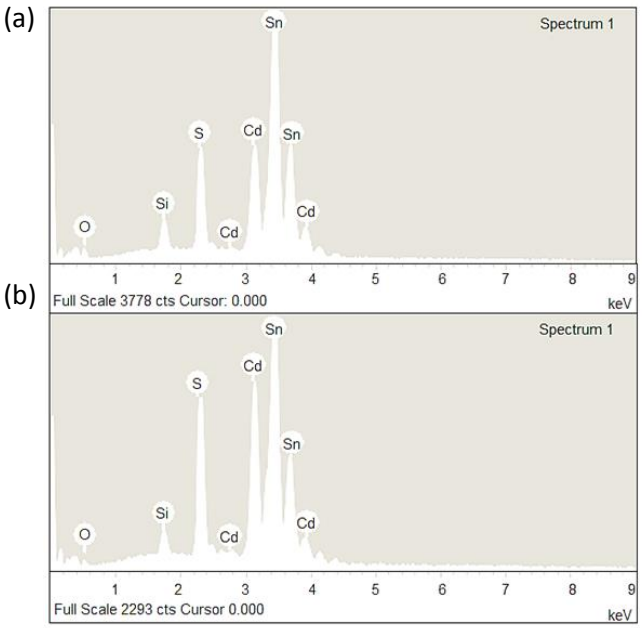

Fig. 5 EDX spectra of (a) as-deposited and (a) heat-treated CdS thin films

The binary phase diagram of the CdS system, adapt from ref [15], is shown in Fig. 6. In this diagram, solid and liquid phases are described. As shown in Fig. 6, the melting point of pure intrinsic CdS is 1405^{o}C. The melting point of Cd is ~ 321 ^{o}C, so all Cd-rich CdS compounds will exhibit some level of liquid phase above ~321^{o}C. Likewise, S-rich CdS shows 2 solid phases, α- and β-. The melting point for α- is at ~95^{o}C and melting point for β- phase is ~115^{o}C. The liquidus temperature of S-rich CdS is observed at 1000^{o}C. On the basis of the phase diagram in Fig. 6, the CdS thin films discussed here have been further studied using different heat-treatment temperatures varying from 250 to 550^{o}C. This was done primarily to provide different crystal growth rates and resulting morphologies but also to provide the possibility of a small amount of partial liquid-phase sintering for any compositions deviating from perfect 50:50 Cd:S stoichiometry, and thereby potentially enabling reduction of pinholes. However, XRD patterns of as-deposited and heat-treated samples (Fig. 2 and 3) show low levels of amorphous component in all samples. It is possible that this may originate from the underlying glass/FTO substrate but it also suggests low levels of amorphous content in the CdS layer. If this was the case, the amorphous humps present in all XRD patterns would indicate that the content of amorphous CdS which was retained during post-processing were comparable at room temperature. However, EDX analysis suggests CdS thin films are slightly enrich in S which would support the presence of some liquid phase at temperatures above 95-115^{o}C, it is noted that EDX is generally not a fully quantitative analysis method. Therefore, whilst there is no direct evidence supporting the involvement of some level of liquid-phase sintering during heat treatment off-stoichiometric Cd:S ratio, it cannot be discounted.

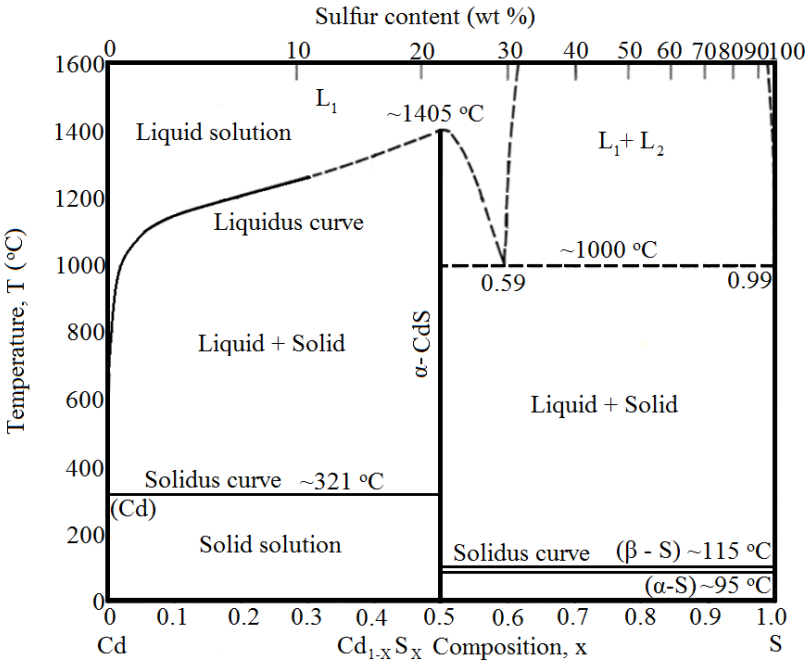

Fig. 6 Phase diagram of CdS

3.4 Optical absorption studies

Optical properties of CdS layers were studied at room temperature by using a UV-Vis spectrophotometry in the wavelength range 200 nm - 1000 nm. Measurements were carried out to study the optical absorbance and transmittance behaviour of CdS layers. Fig. 7 shows the optical absorbance spectra for CdS thin films grown at different voltages for as-deposited and annealed samples. The square of absorbance (A^2) has been plotted as a function of photon energy, and the band gap energy was estimated by extrapolating the straight-line portion of the graph to the photon energy axis. The band gap energy of as-deposited CdS films was found to be scattered from 2.01 to 2.50 eV. It is observed that the band gap energy gradually reduces with an increase in growth voltage, V_g. It is understood that deposition at higher potential enhances the deposition rate of cadmium, resulting in lower band gap [16]. This band gap shift is also clearly consistent with the change of the colour of the CdS thin films as shown in Fig. 8. CdS layers grown at lower growth potentials ($V_g \leq 1445$ mV) show transparent yellow films and as the growth potential increases, the film colour becomes dark green in appearance which demonstrates the effect of Cd- richness. After the heat treatment of the samples at 400^{o}C for 20 min., most of the band gap energies shifted to 2.42 eV, which is equal to the bulk (standard) value for hexagonal CdS.

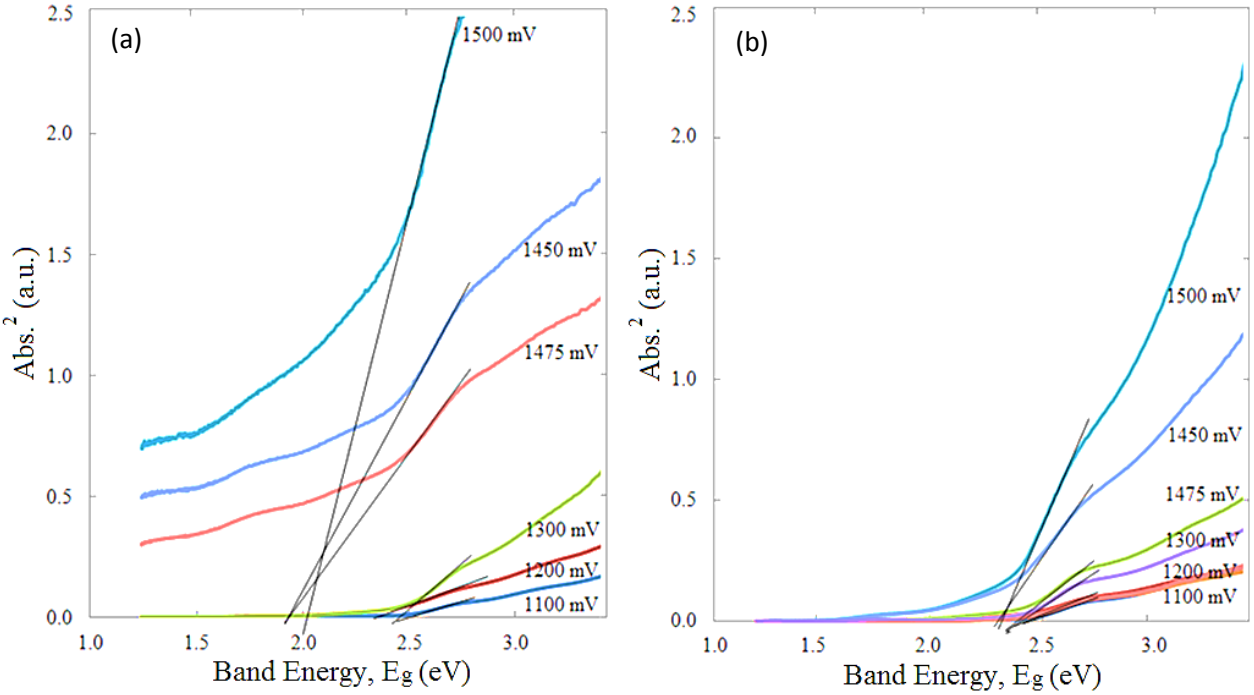

Fig. 7 Optical absorption of CdS thin films grown at different voltages for (a) as-deposited and (b) heat treated samples at 400°C for 20 min. in air

Table 4 Energy band gap of CdS films grown at different growth potentials

	Energy band gap, E_g (eV)											
V_g (mV)	1100	1200	1300	1400	1425	1440	1445	1450	1455	1460	1475	1500
As-deposited	2.50	2.40	2.45	2.45	2.45	2.45	2.40	1.91	2.03	2.10	1.95	2.05
Heat Treated	2.42	2.42	2.42	2.38	2.42	2.45	2.42	2.30	2.42	2.42	2.42	2.32

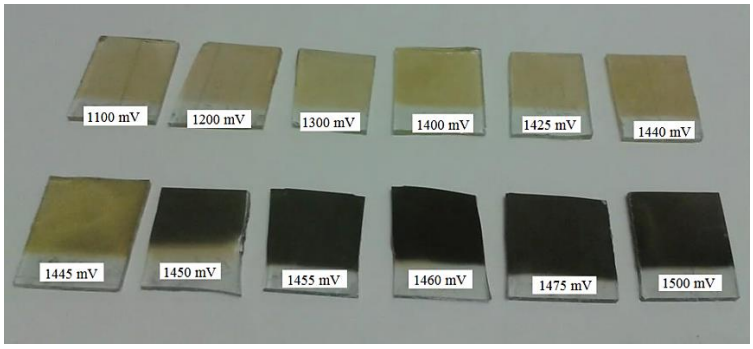

Fig. 8 The physical appearance of as-deposited CdS grown at V_g from 1100 mV to 1500 mV

The CdS optical properties were studied as a function of heat treatment temperature. From Fig. 9(a), it is found that higher heat treatment temperatures result in small absorbance values at the band gap region which could be due to the grain growth. This results in larger unfilled inter-granular volume and consequently the absorption per unit thickness is reduced [9]. The band gap energy is increased as the heat treatment temperature increases. As shown in Fig. 9(b), the samples with higher heat treatment temperature show good transmission (>60%) for wavelength larger than 512 nm, which is one of the criteria for qualification as solar cell window layers [15, 16].

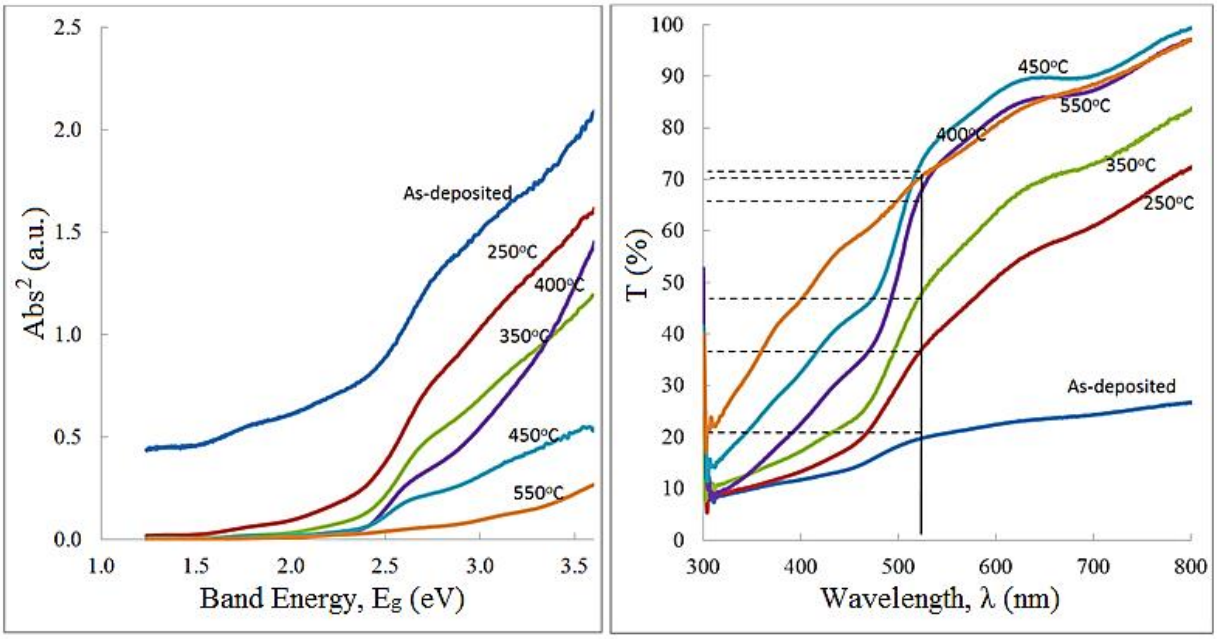

Fig. 9 The variation of (a) Optical absorbance and (b) Optical transmittance of CdS layers with different heat treatment temperatures. The films were grown at 1455 mV

Table 5 The summary of optical properties of CdS films grown at V_g = 1455 mV and heat-treated from 250 to 550°C for 20 min. duration

Heat treatment Temp (°C)	E_g (eV)	T (%)
As-deposited	2.03	19
250	2.25	35
350	2.33	46
400	2.42	66
450	2.42	70
550	2.45	73

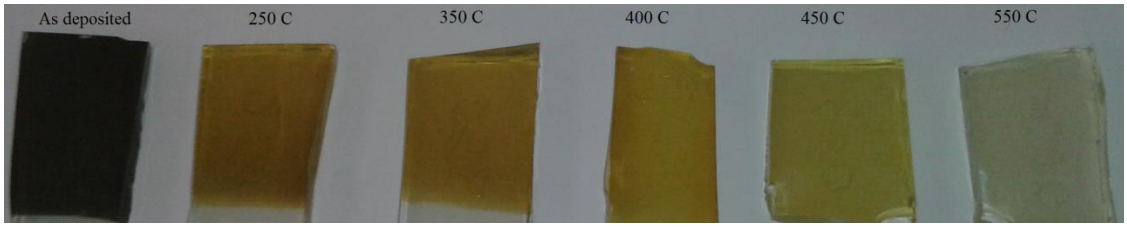

Fig. 10 Appearance of the CdS thin films at different heat-treatment temperatures

Table 5 summarizes the variation of E_g and transmission as the function of heat treatment temperature. Duration of heat treatment was kept constant at 20 min. It is clear that the bandgap reaches 2.42 at 400°C, and then tend to increase. This increase must be due to loss of material through sublimation and thinning down the layer. As a result, the transmission increases and this is also indicated by the appearance change in Fig. 10. Therefore CdS films should only be heat-treated at ~400°C for 20 min. in order to avoid material losses.

3.5 Microstructure and morphological studies

3.5.1 Scanning electron microscopy

Fig. 11 shows the SEM images of as-deposited and heat-treated (at 250, 350, 400, 450 and 550°C for 20 min.) of CdS thin films. It is observed from the SEM images that the as-deposited CdS thin film covers the substrate but with gaps between grains forming clusters of the size about 150-350 nm. The SEM images of heat treated CdS

(Fig. 11(b-f)) show a slight improvement in cluster size and a reduced amount of voids. The heat treatment of these clusters has shown an enhancement of their mean size achieving diameters of 400-550 nm. This is due to coalescence of smaller nano-clusters into larger clusters. The change in microstructure has been attributed to the transformation of a mixed hexagonal and cubic phase into single hexagonal phase (from XRD) after heat treatment as well as re-crystallisation [5, 12].

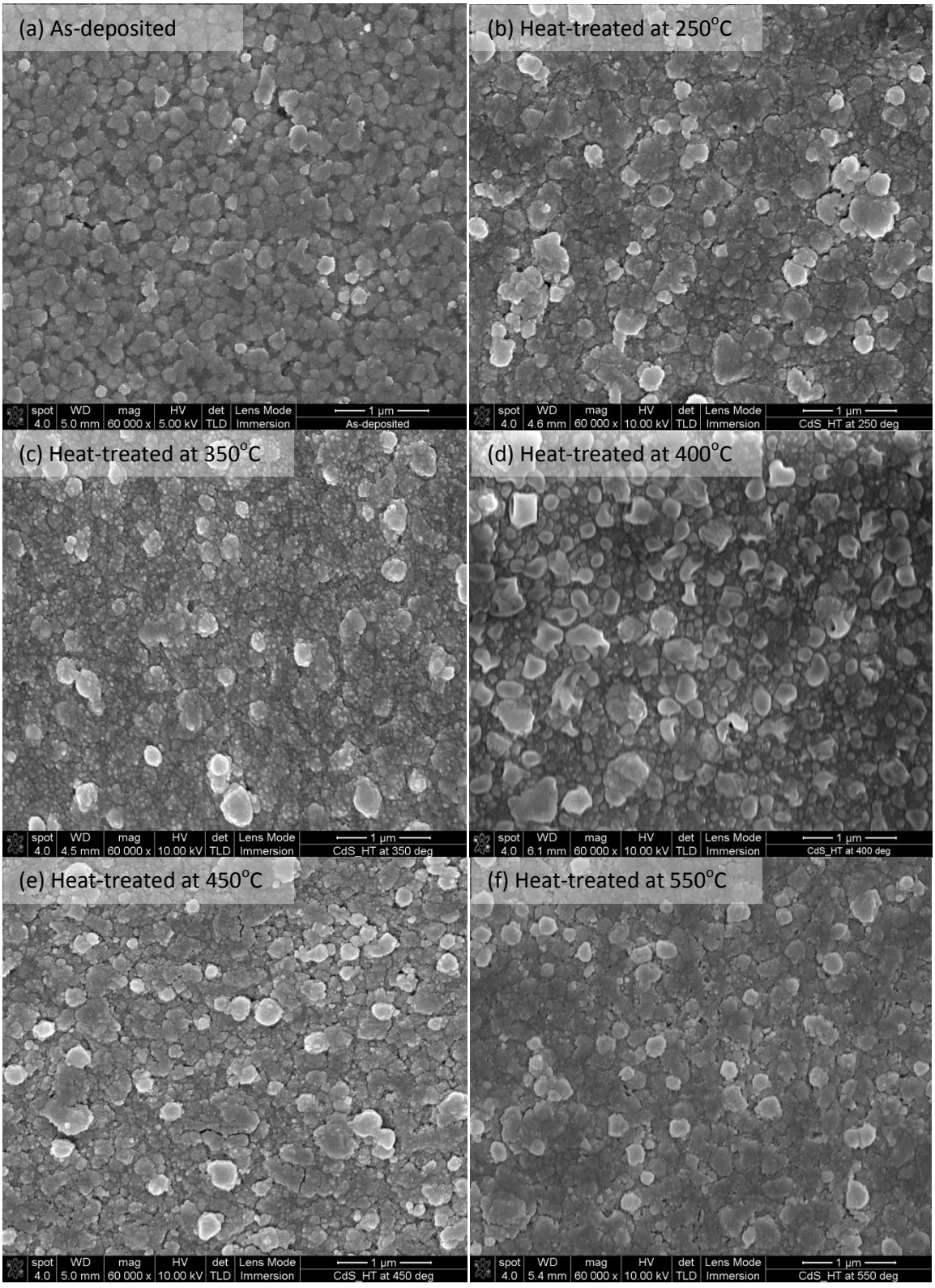

Fig. 11 SEM images of CdS grown at 1455 mV (a) as-deposited and after heat treatment at (b) 250, (c) 350, (d) 400, (e) 450 and (f) 550°C in air for 20 min.

3.5.2 Atomic Force Microscopy

AFM is a convenient technique to study the morphology and surface roughness of thin films. AFM images for as-deposited and heat treated CdS thin films are shown in Fig. 12. The brightness of the images indicates the variation depth of the surface morphology. It is observed from Fig. 12(a), the as-deposited CdS thin film is dense with small grains and less bumpy as compared to the heat-treated CdS. As confirmed by the SEM images in Fig 11, the CdS thin films have larger grains after heat treatment due to the coalescence of small grains. Thus result in valley and bumpy surface along with non-uniform thickness. However, larger grain is good for solar cell device because of having less grain boundaries and ease the electron movement with fewer scattering.

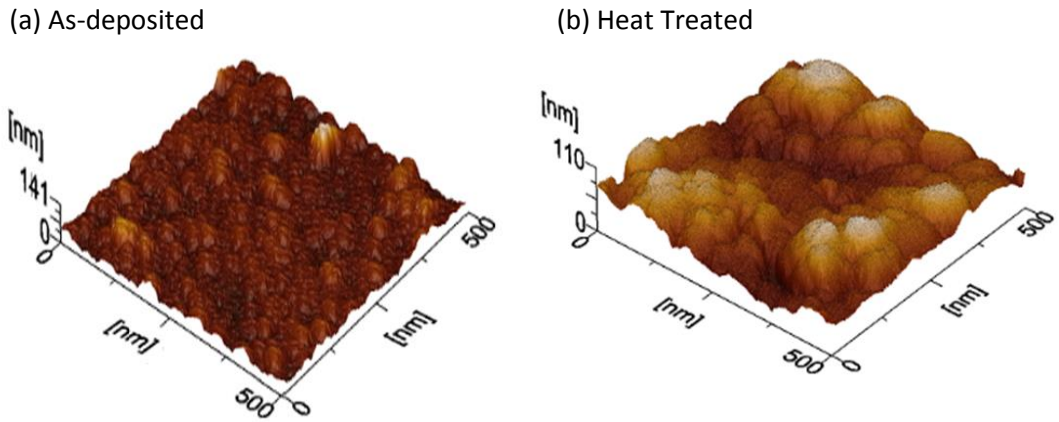

Fig. 12 AFM images of CdS grown at 1455 mV (a) as-deposited and (b) heat-treated layers

3.6 Measurement of electrical properties.

3.6.1 Photoelectrochemical (PEC) cell measurements

The conductivity type of the CdS thin films were determined by PEC cell procedure where CdS film/0.1M $Na_2S_2O_3$ electrolyte formed a solid/liquid Schottky junction. The difference between the measured voltages under dark and illuminated conditions gives the open circuit voltage of the liquid/solid junction. The polarity of the measured voltage determines the electrical conductivity type of the CdS layer. Fig. 13 shows the trend of PEC signal for as-deposited and heat-treated CdS thin films. All these layers were grown at different V_g values. It is observed that all CdS thin films have n-type conductivity for as-deposited and heat-treated samples. About 67% of the PEC signals improve after the heat treatment especially for CdS grown at higher cathodic potentials $V_g > 1300$ mV. This is attributed to the sulphur (S) evaporation during the heat treatment.

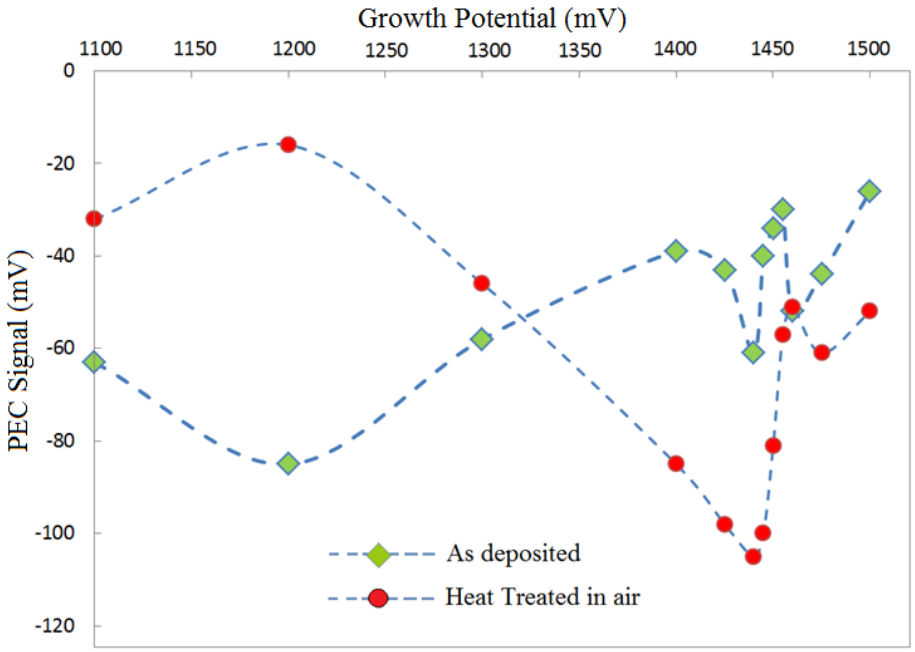

Fig. 13 PEC signals of CdS layers grown at cathodic potential from 1100 mV to 1500 mV, indicating n-type electrical conduction for all layers

3.6.2 D.C. conductivity measurements

D.C. conductivity measurements were carried out in order to determine the electrical conductivity/resistivity of electro-deposited CdS layers. For these experiments, thicker layers were used in order to avoid leakage through pin-holes. 2 mm diameter and circular ohmic contacts were made by evaporating Al through a metallic mask. The resistance of FTO/CdS/Al structures were measured using I-V characteristics. The electrical conductivity (σ) and the resistivity (ρ) were calculated with known thicknesses. The measurements were carried out for CdS layers heat-treated at different temperatures.

Table 6 summarizes the measurements of average resistance, resistivity and electrical conductivity of CdS layers as a function of the heat-treatment temperatures. It shows that the value of conductivity decreases as the CdS films were heat-treated at higher temperature. Many researchers however, reported the increasing in conductivity of CdS after heat treatment [4, 5, 18]. This behaviour is expected in polycrystalline semiconductors due to improvement of crystallinity. However, S. Preusser and M. Cocivera have reported the decreasing in conductivity of CdS after heat treatment [19]. The decrease in conductivity of CdS thin films with higher heat treatment temperature is probably due to the oxidation and diffusion of Na from glass to CdS layer. Heat treatment temperature like 550^{o}C was seen too high for CdS thin films.

Table 6 The summary of electrical properties of CdS thin films heat treated at different temperatures

Heat treatment temperature (^{o}C)	Average Resistance (Ω)	Resistivity, ρ x 10^{5} (Ωcm)	Conductivity, σ x 10^{-6} ($\Omega^{-1}cm^{-1}$)
As deposited	38.37	0.301	33.33
250.0	115.29	1.030	9.67
350.0	188.50	1.692	5.19
400.0	212.01	2.223	4.51
450.0	156.42	2.461	4.07
550.0	396.06	6.252	1.61

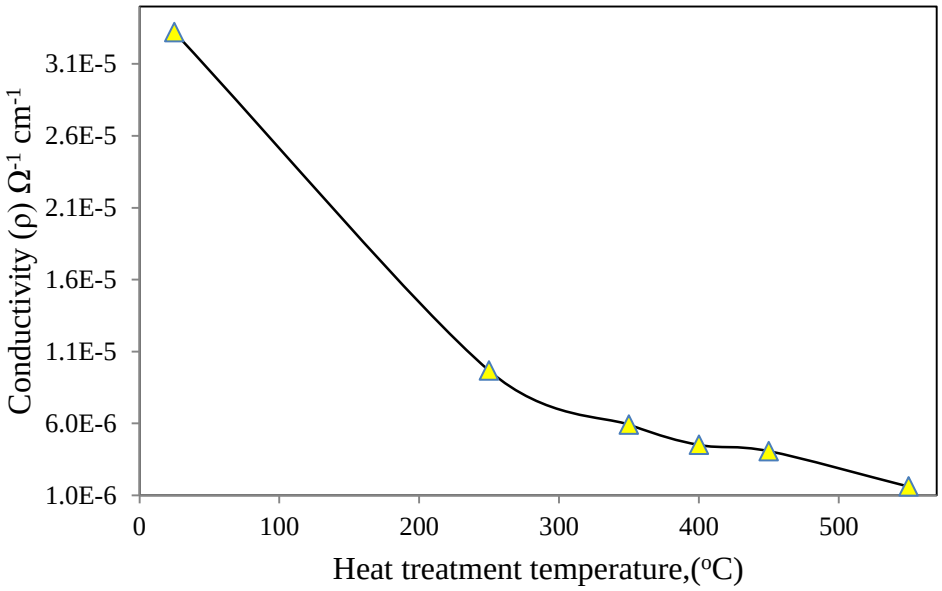

Fig. 14 Electrical conductivity of CdS layers for as-deposited and heat treated at 250, 350, 400, 450 and 550°C, for duration of 20 min

4. CONCLUSION

CdS thin films have successfully grown by electrodeposition from an aqueous electrolyte containing $CdCl_2$ and ammonium thiosulfate ($(NH_4)_2S_2O_3$). Thin films of CdS showed good adhesion to the FTO/glass substrate. XRD studies demonstrated the highest crystallinity after heat treatment in air. The ED-CdS thin films have a polycrystalline structure and these films transform from zinc blend cubic and hexagonal wurtzite mixed phases to a single hexagonal phase after heat treatment in air at 400°C. SEM studies confirm that the formation of large clusters of 150-350 nm for as-deposited layer, growing to 400-550 nm upon heat treatment. The effect of heat treatment brings the energy gap value to the CdS bulk value of 2.42 eV. In summary, CdS thin films electrodeposited at 1455 mV and heat treated at 400°C demonstrates better crystalline quality, band gap similar to its bulk material value, high transmittance, low absorption, low surface roughness and suitable for use as window layers in solar cells fabrication. Incorporating of these layers in device structure is progressing.

ACKNOWLEDGEMENTS

The authors would like to thank P. Bingham, F. Fauzi, H. I. Salim, M. Madugu, O. Olusola and A. Ojo for their valuable contributions. The members at Institute of Organic Catalysis and Electrochemistry, Kazakhstan are acknowledged for their contributions on AFM characterization in this research. The main author would also like to acknowledge the Ministry of Higher Education Malaysia and National Defence University of Malaysia for financial support.

REFERENCES

[1] D. Lincot, M. Fromen and H. Catchet, Advance in Electrochemical Science & Engineering, Vol 6 (John Wiley & Sons, New York, 2008), pp. 118
[2] S.K. Das and G.C. Morris, Solar Energy Materials and Solar Cells 28, 305 (1993)
[3] R.K. Sharma, K. Jain and A.C. Rastogi, Current Applied Physics 3, 199 (2003)
[4] A. Ziabari and F.E. Ghodsi, Solar Energy Materials and Solar Cells 105, 249 (2012)
[5] H. Metin and R. Esen, Journal of Crystal Growth 258, 141 (2003)
[6] A. Hasnat and J. Podder, Journal of Scientific Research 4(1), 11 (2012)
[7] K. Yamaguchi, T. Yoshida, T. Sugiura and H. Minoura, The Journal of Physical Chemistry B 102, 9677 (1998)
[8] D.G. Diso, G.E.A. Muftah, V. Patel and I.M. Dharmadasa, Journal of The Electrochemical Society 157(6), 647 (2010)

[9] M.N. Mammadov, A.S. Aliyev and M. Elrouby, International Journal Thin Film Science Technology 5*3*(2), 43 (2012)
[10] P.C. Hayes and S.H. Algie, Process Principles in Minerals and Materials Production, (1993) http://courses.chem.indiana.edu/c360/documents/redpot.pdf. Accessed 21 May 2014
[11] I. Kaur, D.K. Pandya and K.L. Chopra, Journal of the Electrochemical Society 127(4), 943 (1980)
[12] G. Mustafa, M.R.I. Chowdhury, D.K. Saha, S. Hussain and O. Islam, Dhaka Univ. Journal of Sciences 60(2), 283 (2012)
[13] M. Ichimura, F. Goto and E. Arai, Journal of Applied Physics 85(10), 7411 (1999)
[14] F. C. Campbell, Phase Diagram: Understanding the basics, 1st edn. (ASM International, USA, 2012), pp. 73-81
[15] M. Schulz, W. von der Osten, U. Rossler, O. Madelung, Landolt-Bornstein: Numerical Data and Functional Relationships in Science and Technology 1st edn. (Springer, New York, 1987), pp 33-56
[16] T.L. Chu, S.S. Chu, C. Ferekides, C.Q. Wu, J. Britt and C. Wang, Journal of Applied Physics 70, 7608 (1991)
[17] K. Kitahara, T. Ishii, J. Suzuki, T. Bessyo and N. Watanabe, International Journal of Spectroscopy (2011) doi:10.1155/2011/632139
[18] H. Oumous and H. Hadiri, Thin Solid Films 386(1), 87 (2001)
[19] S. Preusser and M. Cociver, Solar Energy Materials 20(1), 1 (1990)
[20] J. Hiie, T. Dedova, V. Valdna and K. Muska, Thin Solid Films 443, 511 (2006)
[21] A. Romeo, D.L. Baktzner, H. Zogg, C. Vignali and A.N. Tiwari, Solar Energy Materials & Solar Cells 67, 311 (2001)
l COCIVERA